journal

J. Am. Ceram. Soc., 79 [10] 2582-86 (1996)

Phase Equilibria in Rare-Earth Chloride–Fluoride and Rare-Earth Chloride–Magnesium Fluoride Systems

Ram A. Sharma*

Corporate Magnesium Center, General Motors Research & Development Center, Warren, Michigan 48090-9055

Equilibrium phase diagrams for the systems $LaCl_3$–LaF_3, $CeCl_3$–CeF_3, $NdCl_3$–NdF_3, $LaCl_3$–MgF_2, $CeCl_2$–MgF_2, and $NdCl_3$–MgF_2 were determined by differential thermal analysis. A eutectic was observed at 654° ± 4°C and 31 mol% LaF_3 in the $LaCl_3$–LaF_3 system, 620° ± 3°C and 31.5 mol% CeF_3 in the $CeCl_3$–CeF_3 system, 615° ± 5°C and 29 mol% NdF_3 in the $NdCl_3$–NdF_3 system, 723° ± 5°C and 30 mol% MgF_2 in the $LaCl_3$–MgF_2 system, 690° ± 3°C and 26 mol% MgF_2 in the $CeCl_3$–MgF_2 system, and 655° ± 3°C and 26.5 mol% MgF_2 in the $NdCl_3$–MgF_2 system. A compound, $NdCl_3 \cdot NdF_3$, decomposing at 595° ± 5°C, also was observed in the $NdCl_3$–NdF_3 system. On the basis of agreement between the activities calculated by the Temkin model and the Clausius–Clapeyron equation, the melts of the rare-earth (RE) chloride and fluoride consisted of RE^{3+}, Cl^-, and F^-. The melts formed with a rare-earth chloride and magnesium fluoride consisted of RE^{3+}, Mg^{2+}, $RECl_6^{3-}$, and MgF_4^{2-}.

I. Introduction

PHASE diagrams provide a means for elucidating the structural species in molten salt mixtures. For this reason, I and co-workers have determined and published the following phase diagrams: CaI_2–$CaCl_2$, CaI_2–CaF_2, and CaI_2–$MgCl_2$;[1] $MgCl_2$–MgF_2, $CaCl_2$–MgF_2, and NaCl–MgF_2;[2] $NdCl_3$–NaCl, $NdCl_3$–$CaCl_2$, $PrCl_3$–NaCl, and $PrCl_3$–$CaCl_2$;[3] MgF_2–MgO, MgF_2–CaO, and MgF_2–Al_2O_3;[4] and LiCl–KCl eutectic and Li_2S systems.[5] For the same reason, the phase diagrams of $LaCl_3$–LaF_3, $CeCl_3$–CeF_3, $NdCl_3$–NdF_3, $LaCl_3$–MgF_2, $CeCl_3$–MgF_2, and $NdCl_3$–MgF_2 systems are determined in this study.

Phase diagrams also are used to optimize electrolyte compositions used in the production and refining of metals.[6] These electrolytes commonly are made of either fluorides or chlorides. Fluoride melts are more capable of dissolving oxides and cleansing the metals but have high melting points and are harsh on containment materials. The chloride melts have low melting points but lack the above two important properties. The phase diagrams of the present study can provide melts having the good properties of fluoride and chloride melts.

II. Experimental Procedure

(1) Materials

Anhydrous lanthanum fluoride (LaF_3), cerium fluoride (CeF_3), neodymium fluoride (NdF_3), magnesium fluoride (MgF_2), lanthanum chloride ($LaCl_3$), and neodymium chloride ($NdCl_3$), of 99.9% purity, were used to prepare each mixture. They were received in sealed containers and opened in a helium-atmosphere dry box. Anhydrous cerium chloride ($CeCl_3$) was prepared in house from cerium chloride hexahydrate ($CeCl_3 \cdot 6H_2O$) using a procedure described for the preparation of anhydrous neodymium chloride from neodymium chloride hexahydrate, $NdCl_3 \cdot 6H_2O$.[7] In this procedure, the cerium chloride hexahydrate was heated slowly in air to ~200°C, until all of the low-temperature water of crystallization was removed. The product was heated slowly in a silica reactor under flowing hydrochloric acid (HCl) to ~450°C and kept at this temperature for ~2 h before cooling to room temperature. The reactor was opened in the helium-atmosphere dry box, and the anhydrous cerium chloride was transferred to a mason jar. Anhydrous neodymium chloride also was prepared for some of the samples by this technique. The material behaved similar to material of 99.9% purity from a different source.

(2) Differential Thermal Analysis

The instrument (Model DTA 1700 System coupled with a System 7/4 Controller and Model 3600 Data Station, Perkin-Elmer, Norwalk, CT) has been used and described in an earlier publication.[3] The instrument consisted of the following: a small resistance-heated furnace, suitable for use up to 1500°C; an alumina enclosure covering the sample and reference containers, for maintaining an argon inert atmosphere; and a device for recording and plotting the differential temperature between the sample and an alumina powder reference versus the sample temperature. Platinum–platinum-10% rhodium thermocouples, which have an accuracy of 3°C in the range of temperatures studied, were used for temperature measurements. A small graphite container with a tight plug (Fig. 1), for holding the sample, and a small alumina container, for holding the reference alumina powder, were used. The containers were fitted atop alumina-sheathed thermocouples.

Various salt compositions were prepared by taking weighed amounts of the components and mixing them in an agate mortar. The accuracy of the mixtures so prepared was checked by induc-

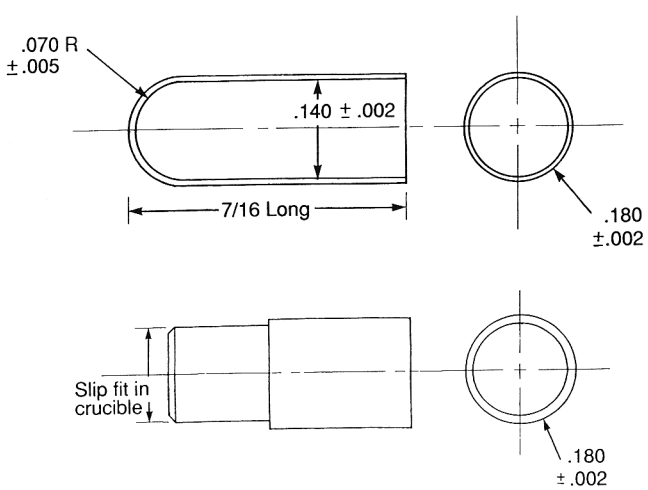

Fig. 1. Schematic sketch of graphite container.

R. Roth—contributing editor

Manuscript No. 192343. Received September 18, 1995; approved March 4, 1996.
*Member, American Ceramic Society.

tively coupled plasma/atomic emission spectroscopy (ICP/AES) chemical analysis, which indicated they were within ±1% of the intended composition. Approximately 80–120 mg of the mixture was placed in the graphite container. The entire operation was performed in a helium-atmosphere glove box. The container with the sample was removed from the glove box in a sealed glass jar. This sample container was removed from the jar and exposed to the atmosphere only for the short time necessary to position it atop the thermocouple and cover it with the alumina enclosure, where it was purged with argon. Phase-transition temperatures were obtained with heating and cooling rates from 1°C/min to 15°C/min.

Typical differential thermal analysis (DTA) curves for a melt of 59.4 mol% $LaCl_3$ and 40.6 mol% LaF_3, at a rate of 10°C/min, are shown in Figs. 2(a) and (b). The transition temperatures are indicated clearly by the changes in the DTA curves. By combining the measurements from the heating and cooling curves, the liquidus temperatures could be determined with good accuracy. The uncertainty could be reduced further by acquiring the measurements at different heating and cooling rates.

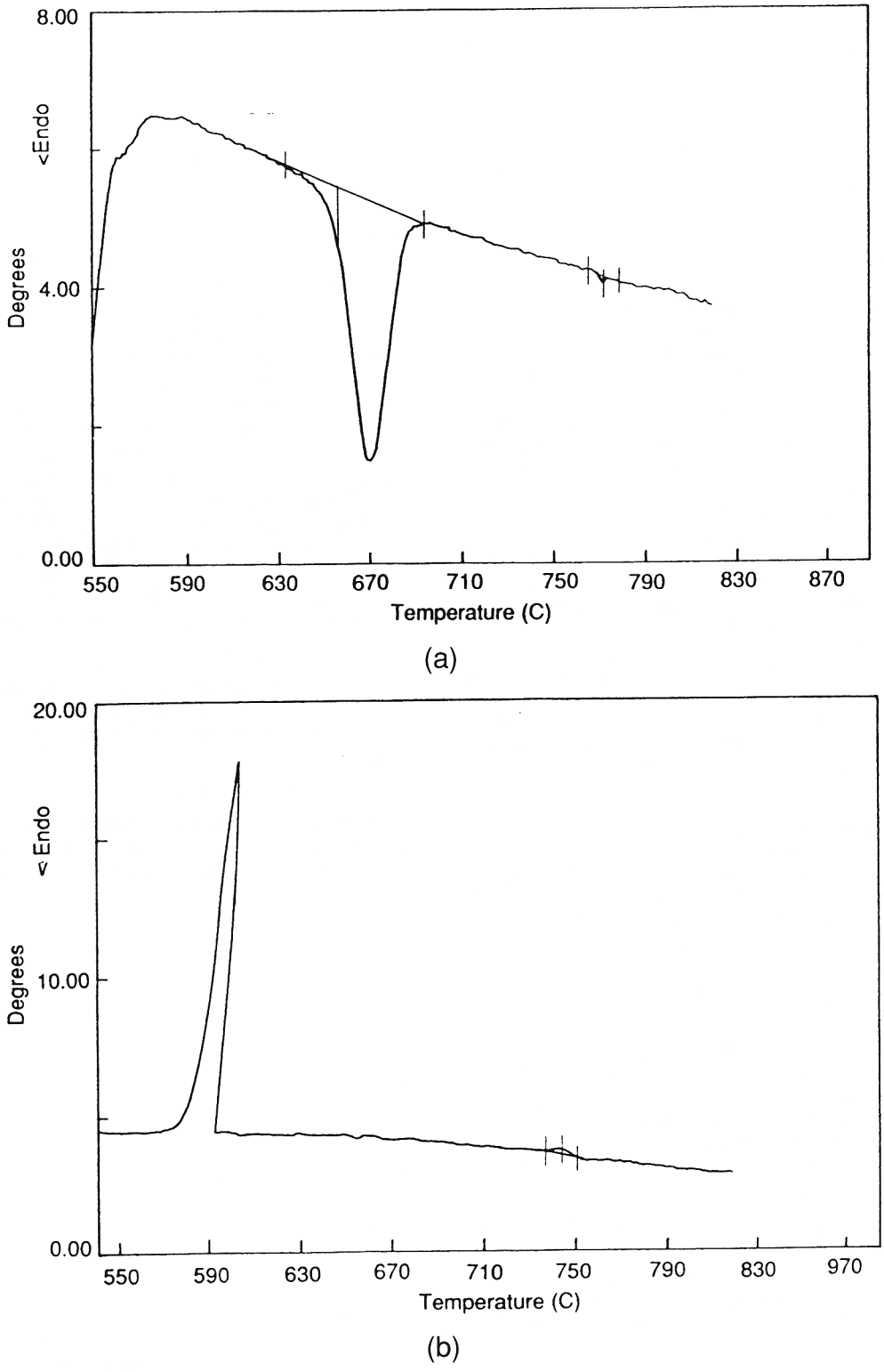

Fig. 2. Typical representation of the DTA (a) heating curve and (b) cooling curve obtained for a melt of 59.4 mol% $LaCl_3$ and 40.6 mol% LaF_3 (heating/cooling rate = 10°C/min, weight = 97.00 mg, and flowing argon atmosphere (20 cm^3/min)).

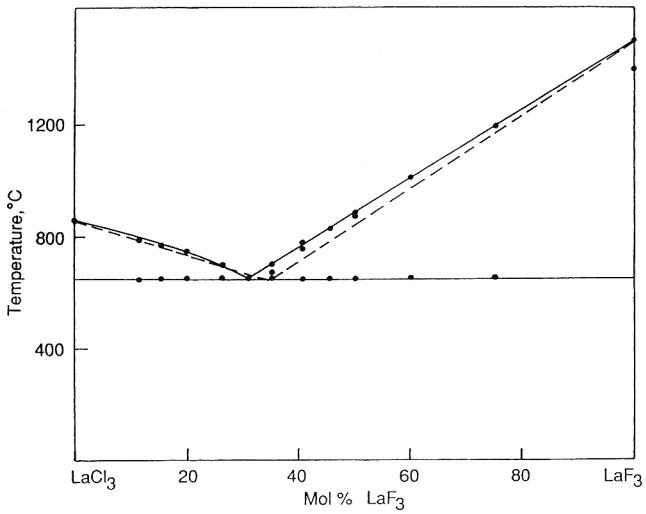

Fig. 3. $LaCl_3$–LaF_3 system.

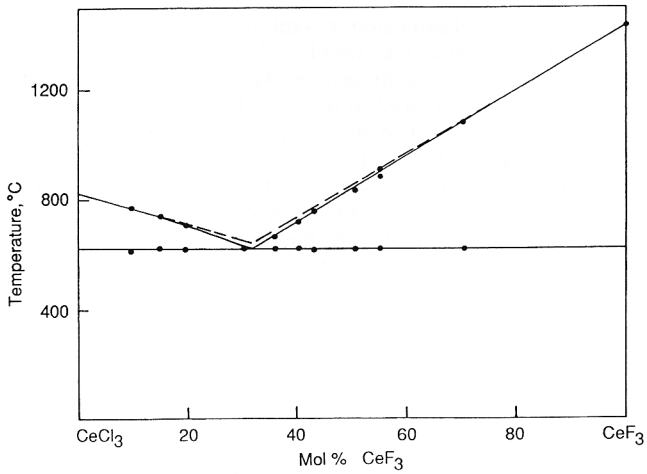

Fig. 4. $CeCl_3$–CeF_3 system.

III. Results and Discussion

The DTA data obtained from the heating and cooling curves are presented in the following tables and figures. The eutectic and liquidus temperatures of the $LaCl_3$–LaF_2 (Table I), $CeCl_3$–CeF_3 (Table II), $NdCl_3$–NdF_3 (Table III), $LaCl_3$–MgF_2 (Table V), $CeCl_3$–MgF_2 (Table VI), and $NdCl_3$–MgF_2 (Table VII) systems have been archived.* Rare-earth chloride and magnesium fluoride in the melts with ~75 mol% or greater magnesium fluoride appeared to react to some extent, forming rare-earth fluoride and magnesium chloride. The reaction was indicated by a ternary peak in the DTA curve and a reduced liquidus temperature. Therefore, the measurements were restricted to <75 mol% magnesium fluoride. Most of the eutectic melts supercooled 100°–150°C. The supercooling was observed from the sharp deflection of the DTA curve and the temperature increase during solidification of the melt. More weight was given to the measurements obtained from the heating curves, and the eutectic temperatures reported are based mostly on these heating measurements. Measured temperatures of the obviously supercooled eutectic melts are reported only to show the extent of supercooling. The accuracy of the thermocouples was checked frequently by using an NaCl sample as a standard.

(1) $LaCl_3$–LaF_3 System

The equilibrium phase diagram based on these measurements is given in Fig. 3. The system has a eutectic at 654° ± 4°C (average of 33 measurements) and a composition containing 31 mol% LaF_3. The eutectic temperature also was possible to obtain from the cooling curves for compositions having more $LaCl_3$ than the eutectic composition.

(2) $CeCl_3$–CeF_3 System

The equilibrium phase diagram based on these measurements is shown in Fig. 4. The melting point of $CeCl_3$ was determined to be 820° ± 1°C, which is higher than that reported in the literature.[8–11] In fact, the melting point of 820°C may even be a few degrees lower, because the $CeCl_3$ used in these measurements had ~1 wt% CeOCl, as indicated by chemical analysis. The system has a simple eutectic at 620° ± 3°C (average of 29 values) and a composition containing 31.5 mol% CeF_3.

(3) $NdCl_3$–NdF_3 System

The equilibrium phase diagram based on these measurements is presented in Fig. 5. The system shows a compound, $NdCl_3 \cdot NdF_3$, decomposing at 595° ± 5°C (average of 39 measurements) to solid $NdCl_3$ and solid NdF_3 below the eutectic temperature. A sample of 50 mol% $NdCl_3$ and 50 mol% NdF_3 was prepared for X-ray diffraction (XRD) analysis by mixing stoichiometric amounts of $NdCl_3$ and NdF_3 in an agate mortar in a helium-atmosphere dry box. The mixture was placed in a graphite crucible, heated to 550°C, and held for 5 d at this temperature before slowly being cooled to room temperature. The sintered sample was powdered in an agate mortar and loaded in an aluminum mount covered with Mylar™ (DuPont, Wilmington, DE) for X-ray analysis inside a helium-atmosphere dry box. The X-ray analysis data are given in Table IV. The XRD pattern differed from those of $NdCl_3$ and NdF_3 and provided evidence for the existence of a compound. The *hkl* values for the three strongest lines—4.2823 Å (18.92%), 3.4214 Å (100%), and 2.4597 Å (9.58%)—are [002], [400], and [223], respectively, and the tetragonal unit-cell dimensions of the sintered sample are $a = b = 13.695$ Å and $c = 8.566$. A eutectic in the system is observed at 615° ± 5°C (average of 29 measurements) and a composition containing 29 mol% NdF_3.

(4) $LaCl_3$–MgF_2 System

The equilibrium phase diagram based on these measurements is presented in Fig. 6. The system has a eutectic at 723° ± 5°C (average of 19 values) and a composition containing 30 mol% MgF_2.

(5) $CeCl_3$–MgF_2 System

The equilibrium phase diagram based on these measurements is presented in Fig. 7. The system has a eutectic at 690° ± 3°C (average of 23 values) and a composition containing 26 mol% MgF_2.

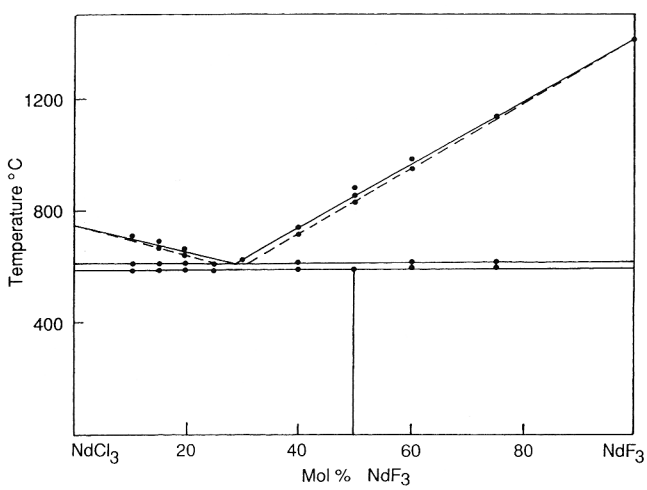

Fig. 5. $NdCl_3$–NdF_3 system.

*For Tables I–III and V–VII, order ACSDD-249 from Data Depository Services, American Ceramic Society, 735 Ceramic Place, Westerville, OH 43081–8720.

Table IV. XRD Data of Powdered $NdCl_3 \cdot NdF_3$ Compound

2θ (degrees)	Lattice spacing, d (Å)	Intensity (cps)	Amount (%)
20.307	4.3695	66.86	16.94
20.725	4.2823	74.67	18.92
26.022	3.4214	394.69	100.00
33.348	2.6846	20.16	5.11
34.773	2.5778	21.84	5.53
36.499	2.4597	37.82	9.58
40.492	2.2259	12.74	3.23
41.407	2.1788	23.65	5.99
42.251	2.1372	28.78	7.29
47.475	1.9135	10.55	2.67
49.636	1.8352	11.98	3.04
52.492	1.7418	15.80	4.00
52.956	1.7276	10.99	2.79
65.506	1.4238	13.08	3.31
66.938	1.3967	8.33	2.11
70.096	1.3413	10.67	2.70
77.553	1.2299	9.08	2.30

(6) $NdCl_3$–MgF_2 System

The equilibrium phase diagram based on these measurements is presented in Fig. 8. The system has a eutectic at 655° ± 3°C (average of 22 measurements) and a composition containing 26.5 mol% MgF_2.

(7) Ionic Species in the Melts

The method adopted here to ascertain the ionic species in the melts and to use them in constructing the phase diagrams is to assume certain ionic species in a melt and calculate the activities of the melt components using the Temkin model.[12] According to this model, the activity of a component in a melt is equal to the product of its cationic and anionic fractions.[12] The calculated activities are compared to those calculated using the Clausius–Clapeyron equation. If the activities calculated by the two methods agree, then the assumed ionic species are considered to be correct. The phase diagram is constructed using the relations between mole fractions, ionic fractions, and the activities at different temperatures. For example, $LaCl_3$–LaF_3 melts are assumed to consist of La^{3+}, Cl^-, and F^-. According to the Temkin model, the activity of $LaCl_3$ in the $LaCl_3$–LaF_3 melt, a_{LaCl_3}, is given as

$$a_{LaCl_3} = X_{La^{3+}} X_{Cl^-}^3 \tag{1}$$

where X is the ionic fraction of the designated ion or the mole fraction of the salt. Then,

$$X_{La^{3+}} = 1 \tag{2}$$

and

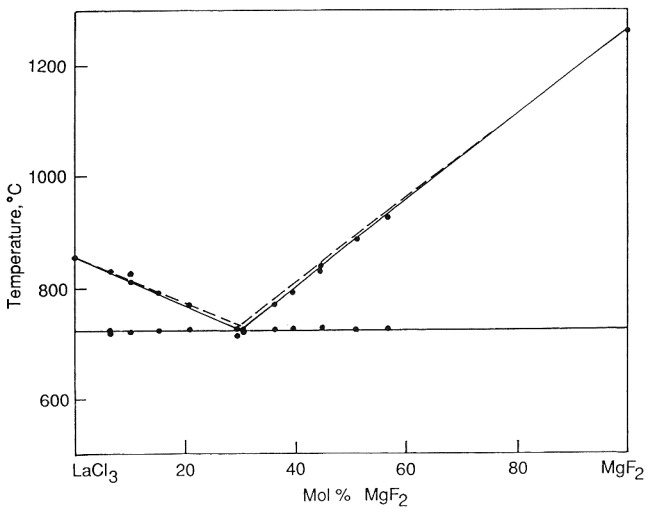

Fig. 6. $LaCl_3$–MgF_2 system.

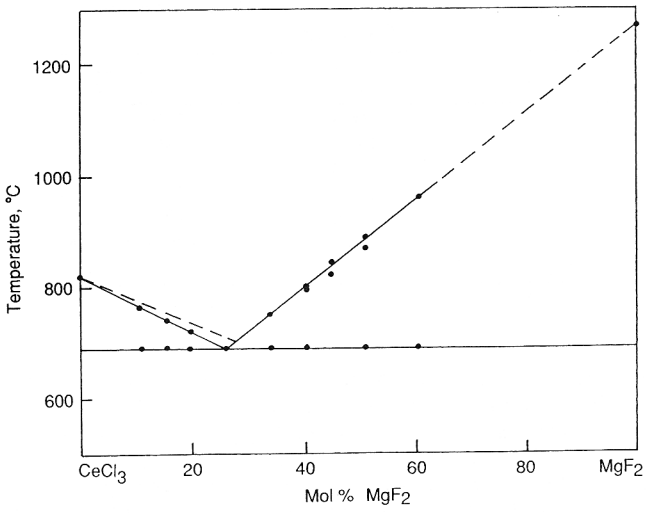

Fig. 7. $CeCl_3$–MgF_2 system.

$$X_{Cl^-} = \frac{3X_{LaCl_3}}{3X_{LaCl_3} + 3X_{LaF_3}} = X_{LaCl_3} \tag{3}$$

Therefore, as per the model,

$$a_{LaCl_3} = X_{LaCl_3}^3 \tag{4}$$

and, similarly, the activity of LaF_3 is given as

$$a_{LaF_3} = X_{LaF_3}^3 \tag{5}$$

The activity of $LaCl_3$ also is calculated by using a simplified Clausius–Clapeyron equation as follows:

$$\log a_{LaCl_3} = -\frac{\Delta H_M}{R}\left(\frac{1}{T} - \frac{1}{T_M}\right) \tag{6}$$

where ΔH_M is the heat of fusion, R the gas constant, T_M the melting point, and T the absolute temperature under consideration. Numerical values of these quantities are given in Table VIII.

Using the calculated value of activity in Eq. (4), the mole fraction of $LaCl_3$ can be calculated at the temperature of interest. Similarly, the mole fraction of LaF_3 can be calculated, and the mole fractions of $LaCl_3$ and LaF_3 can be used for calculating the liquidii in the melt. The liquidii shown by dashed lines in Fig. 3 have been calculated as described above. The agreement

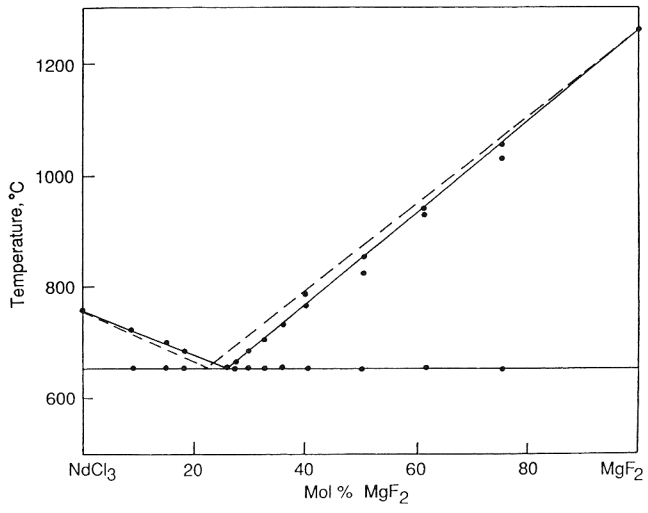

Fig. 8. $NdCl_3$–MgF_2 system.

Table VIII. Melting Points and Heats of Fusion for Components*

Compound	Melting point, T_M (K)	Heat of fusion, ΔH_M (cal/mol)
$CeCl_3$	1093	12800 ± 400
$LaCl_3$	1128	1300 ± 200
$NdCl_3$	1023	11600
CeF_3	1710	13500 ± 2500
LaF_3	1766	1200 ± 200
NdF_3	1673	13080 ± 200
MgF_2	1536	13900 ± 200

*From Refs. 9 and 10.

between the measured and the calculated liquidii is reasonable and indicates the assumed ionic species are correct.

The melts of the $CeCl_3$–CeF_3 system are assumed to consist of Ce^{3+}, Cl^-, and F^-, and those of the $NdCl_3$–NdF_3 system are assumed to consist of Nd^{3+}, Cl^-, and F^-. Proceeding as in the case of the $LaCl_3$–LaF_3 system and using the data given in Table VIII, the liquidii in these systems have been calculated and are presented as dashed lines in Figs. 4 and 5, respectively. In these systems also, the agreement between the measured and calculated liquidii is reasonable. This agreement, and that in the case of $LaCl_3$–LaF_3 system, indicates that the melts of each of these three systems consist of the respective simple rare-earth cations Cl^-, and F^-.

Proceeding as in the above three systems, the liquidii were calculated for the $LaCl_3$–MgF_2, $CeCl_3$–MgF_2, and $NdCl_3$–MgF_2 systems, assuming the melts of each system to consist of simple rare-earth ions Mg^{2+}, Cl^-, and F^-. No agreement was found between the calculated and the measured liquidii, indicating these melts consisted of different combinations of ions than postulated. On the other hand, the liquidii shown by dashed lines in Figs. 6–8 were produced from the mole fractions of the respective components considered to be square roots of the activities calculated by the Clausius–Clapeyron equation at the temperatures under consideration. In each case, the agreement between the calculated and measured liquidii is reasonable. This leads to the following conjecture: the melts of $LaCl_3$–MgF_2 consist of La^{3+}, Mg^{2+}, $LaCl_6^{3-}$, and MgF_4^{2-}; those of $CeCl_3$–MgF_2 consist of Ce^{3+}, Mg^{2+}, $CeCl_6^{3-}$, and MgF_4^{2-}; and those of $NdCl_3$–MgF_2 consist of Nd^{3+}, Mg^{2+}, $NdCl_6^{3-}$, and MgF_4^{2-}.

Acknowledgments: The author is thankful to Mark W. Verbrugge and Kathleen C. Taylor for their support, valuable discussions, and review of the manuscript. The author also would like to thank M. Ahsan Habib and Randall N. Seefurth for assistance with the DTA work and Andrew M. Wims of the Analytical Chemistry Department, General Motors Research and Development Center, for the X-ray analysis.

References

[1]R. A. Sharma, "Liquidus and Eutectic Phase Equilibria in the Systems CaI_2–$CaCl_2$, CaI_2–CaF_2, CaI_2–$MgCl_2$," *High Temp. Sci.*, **1** [4] 423–29 (1969).

[2]R. A. Sharma and I. Johnson, "Phase Diagrams for the Systems $MgCl_2$–MgF_2, $CaCl_2$–MgF_2," *J. Am. Ceram. Soc.*, **52** [11] 612–15 (1969).

[3]R. A. Sharma and R. A. Rogers, "Phase Equilibria and Structural Species in $NdCl_3$–NaCl, $NdCl_3$–$CaCl_2$, $PrCl_3$–NaCl, and $PrCl_3$–$CaCl_2$ Systems," *J. Am. Ceram. Soc.*, **75** [9] 2484–90 (1992).

[4]R. A. Sharma, "Phase Equilibria and Structural Species in MgF_2–MgO, MgF_2–CaO, and MgF_2–Al_2O_3 Systems," *J. Am. Ceram. Soc.*, **71** [4] 272–76 (1988).

[5]R. A. Sharma, "Phase Diagram of Pseudo-Binary LiCl–KCl Eutectic and Li_2S System," *J. Electrochem. Soc.*, **133** [5] 859–62 (1986).

[6]C. L. Mantell, *Electrochemical Engineering*, 4th Ed. McGraw-Hill, New York, 1960.

[7]G. J. Kipouros and R. A. Sharma, "Preparation of High-Purity Anhydrous Neodymium Chloride"; pp. 43–55 in *Rare Earths, Resources, Science, Technology and Applications*. Edited by R. G. Bautista and N. Jackson. Minerals, Metals, and Materials Society, Warrendale, PA, 1991.

[8]O. Kubaschewski and C. B. Alcock, *Metallurgical Thermochemistry*, 5th Ed. Pergamon, Elmsford, NY, 1979.

[9]I. Barin, O. Knacke, and O. Kubaschewski, *Thermo-Chemical Properties of Inorganic Substances*. Springer-Verlag, Berlin, FRG, 1973.

[10]*JANAF Thermochemical Tables*, 2nd Ed.; No. NSRDS-NBS-37. Edited by D. R. Stull and H. Prophet. U.S. Government Printing Office, Washington, D.C., 1971.

[11]*Handbook of Chemistry and Physics*, 67th Ed.; p. B-104. CRC Press, Boca Raton, FL.

[12]M. Temkin, "Mixtures of Fused Salts as Ionic Melts," *Acta Physicochim URSS*, **20**, 411–20 (1945). □